Chemistry Research Journal, 2019, 4(1):46-59

Available online www.chemrj.org

Research Article

ISSN: 2455-8990
CODEN(USA): CRJHA5

An introductory theoretical investigation of the relationships between electronic structure and A_1, A_{2A} and A_3 adenosine receptor affinities of a series of N^6-8,9-trisubstituted purine derivatives.

Juan S. Gómez-Jeria*, Bruno Sánchez-Jara

Quantum Pharmacology Unit, Department of Chemistry, Faculty of Sciences, University of Chile. Las Palmeras 3425, Santiago 7800003, Chile

Abstract A study of the relationships between receptor affinity and electronic structure was performed in a group of N^6-8,9-trisubstituted purine derivatives interacting with A_1, A_{2A} and A_3 adenosine receptors. Statistically significant equations were obtained for all cases.

Keywords QSAR, common skeleton, DFT, electronic structure, pharmacophore, purine derivatives, adenosine receptors, KPG method, receptor affinity, purine

Introduction

Adenosine is a pervasive molecule involved in the regulation of the function of each tissue and organ. It affects nearly all aspects of cellular physiology, such as blood cell regulation, neuronal activity, platelet aggregation, stimulation of glutamate release from astrocytes and vascular function. This molecule mediates its effects through the activation of a family of four G-protein coupled adenosine receptors, called A_1, A_{2A}, A_{2B} and A_3 [1-8]. Adenosine antagonists have stimulant and anxiogenic effects although adenosine agonists have sedative, anticonvulsant and anxiolytic actions. This fact prompted the synthesis and testing of many groups of molecules interacting with one or more adenosine receptors [2-4, 6, 9-25]. Some theoretical studies were carried out[16, 25, 26, 27]. Given the pharmacological interest of these molecules, we become interested in testing again the validity of the formal Klopman-Peradejordi-Gómez method to find significant structure-activity relationships.

Here we present the results of a theoretical analysis of the relationships between molecular/electronic structure and receptor affinity for a group of N^6-8,9-trisubstituted purine derivatives interacting with A_1, A_{2A} and A_3 adenosine receptors.

Molecules and calculations

The molecules and receptor affinity results were taken from a recent publication, and are presented in Fig. 1 and Table 1[9].

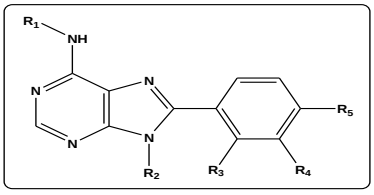

Figure 1: General formula of molecules used in this study

Table 1: N^6-8,9-trisubstituted purine derivatives and their receptor affinities.

Mol.	R_1	R_2	R_3	R_4	R_5	$\log(K_i)$ A_1AR	$\log(K_i)$ $A_{2A}AR$	$\log(K_i)$ A_3AR
1	H	Me	H	H	H	1.36	2.58	4.15
2	H	Et	H	H	H	1.49	2.33	3.76
3	H	Pr	H	H	H	2.00	2.69	3.97
4	*c*-butyl	Me	H	H	H	0.51	2.48	2.45
5	*c*-butyl	Et	H	H	H	0.78	2.58	1.92
6	*c*-butyl	Pr	H	H	H	1.18	2.56	2.42
7	*c*-pentyl	Me	H	H	H	0.45	2.70	2.93
8	*c*-pentyl	Et	H	H	H	0.59	2.52	2.55
9	*c*-pentyl	Pr	H	H	H	1.00	2.80	2.87
10	3-$(CH_2)_4O$	Me	H	H	H	0.90	3.26	3.80
11	3-$(CH_2)_4O$	Et	H	H	H	1.00	3.01	3.22
12	3-$(CH_2)_4O$	Pr	H	H	H	1.40	3.23	3.45
13	*c*-hexyl	Me	H	H	H	0.76	2.72	3.37
14	*c*-hexyl	Et	H	H	H	1.00	2.49	2.85
15	*c*-hexyl	Pr	H	H	H	1.43	3.03	3.37
16	*c*-pentyl	Me	---	H	H	2.38	3.80	4.04
17	*c*-pentyl	Me	Me	H	H	1.74	3.84	3.48
18	*c*-pentyl	Me	H	Me	H	0.79	2.65	2.71
19	*c*-pentyl	Me	H	H	Me	0.90	3.26	2.68
20	*c*-pentyl	Me	Cl	H	H	1.57	3.49	2.86
21	*c*-pentyl	Me	H	H	Cl	1.26	3.26	3.08
22	*c*-pentyl	Me	H	H	F	0.79	3.38	3.06
23	*c*-pentyl	Me	H	H	OMe	1.88	3.25	3.27
24	*c*-pentyl	Me	H	H	OH	1.23	2.73	2.72
25	*c*-pentyl	Me	H	H	COOH	4.73	---	4.41

Calculations [28]

The formal relationship between electronic structure and receptor affinity was developed many years ago and it is known as the Klopman-Peradejordi-Gómez method (KPG method). Its theoretical foundations are well known and have been reviewed in detail [29-36]. The application of the KPG method to different chemical systems and biological activities has been very successful [37-58].

The electronic structure of all molecules was calculated within the Density Functional Theory (DFT) at the B3LYP/6-31G(d,p) level with full geometry optimization [59]. The Gaussian suite of programs was used [59]. The information needed to calculate the numerical values for the LARIs was obtained from the Gaussian results with the D-Cent-QSAR software [60]. All the electron populations smaller than or equal to 0.01 e were considered as zero. Negative electron populations coming from Mulliken Population Analysis were corrected as usual [61]. Orientational parameters taken from published Tablesor calculated in our Unit with the Steric software [62]. We employed Linear Multiple Regression Analysis (LMRA) techniques to find the best solution. For each case, a matrix containing the dependent variable and the local atomic reactivity indices of all atoms of the common skeleton as independent variables was built. The orientational parameters of the R1-R5 substituents were added. The Statistica software was used for LMRA [63]. The common skeleton numbering is shown in Fig. 2.

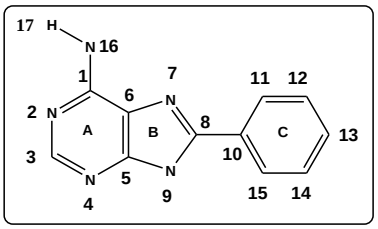

Figure 2: Common skeleton numbering

Results

Results for A_1AR receptors

The best statistically significant equation obtained is the following:

$$\log(K_i)=-7.69+5.61\omega_9-4.50S_6^E(\text{HOMO-1})^*+0.002\phi_{R2}-0.33S_{14}^E(\text{HOMO-2})^* \quad (1)$$

with n=22, adj-R^2=0.96, F(4,17)=139.23 (p<0.000001) and a standard error of the estimate of 0.17. No outliers were detected and no residuals fall outside the ±2σ limits. Here, ω_9 is the local atomic electrophilicity of atom 9, S_6^E(HOMO-1)* is the electrophilic superdelocalizability of the second highest MO localized on atom 6, $\boldsymbol{\varphi_{R2}}$orientational effect of the R_2 substituent and S_{14}^E(HOMO-2)* is the electrophilic superdelocalizability of the third highest molecular orbital localized on atom 14 (see Fig. 2).Tables 2 and 3 show the beta coefficients, the results of the t-test for significance of variable and the matrix of squared correlation coefficients for the variables of Eq. 1. There are no significant internal correlations between independent variables (Table 3). Figure 3 displays the plot of observed *vs.* calculated $\log(K_i)$.

Table 2: Beta coefficients and t-test for significance of coefficients in Eq. 1.

	Beta	t(17)	p-level
ω_9	0.94	21.19	0.000000
S_6^E(HOMO-1)*	-0.44	-10.60	0.000000
φ_{R2}	0.25	5.65	0.00003
S_{14}^E(HOMO-2)*	-0.21	-4.80	0.0002

Table 3: Matrix of squared correlation coefficients for the variables in Eq. 1

	ω_9	**S_6^E(HOMO-1)***	**φ_{R2}**	**S_{14}^E(HOMO-2)***
ω_9	1.00			
S_6^E(HOMO-1)*	0.00	1.00		
φ_{R2}	0.07	0.00	1.00	
S_{14}^E(HOMO-2)*	0.02	0.00	0.04	1.00

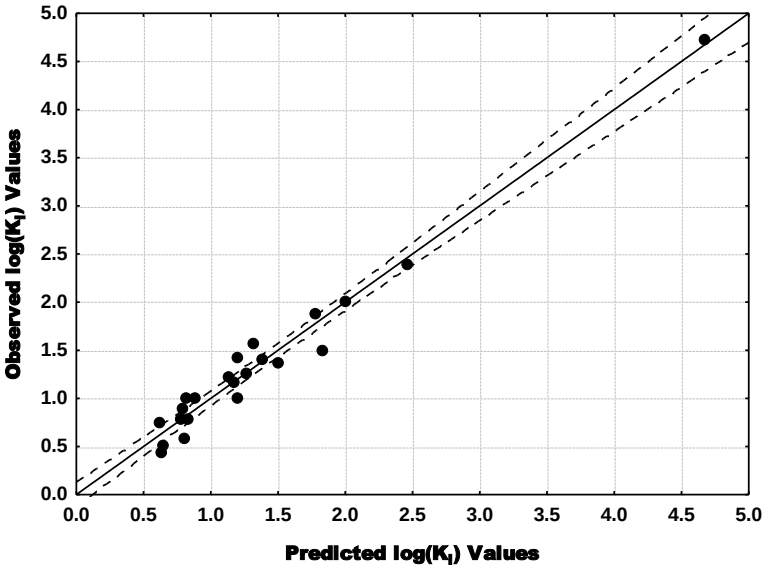

Figure 3: Plot of predicted vs. observed log(K_i). values (Eq. 1). Dashed lines denote the 95% confidence interval

The associated statistical parameters of Eq. 1 indicate that this equation is statistically significant and that the variation of the numerical values of a group of four local atomic reactivity indices of atoms of the common skeleton

explains about 96% of the variation of $\log(K_i)$. Figure 3, spanning about 4 orders of magnitude, shows that there is a good correlation of observed *versus* calculated values.

Results for A_{2A}AR receptors

The best statistically significant equation obtained is the following:

$$\log(K_i)=30.13+1.51S_{15}^{E}+0.44S_{2}^{E}(\text{HOMO-1})^{*}+23.79Q_2+0.09S_{7}^{N}(\text{LUMO+2})^{*} \quad (2)$$

with n=23, R=0.94, R^2=0.89, adj-R^2=0.87, F(4,18)=36.40 ($p<0.000001$) and a standard error of the estimate of 0.16. No outliers were detected and no residuals fall outside the ±2σ limits. Here, S_{15}^{E} is the total atomic electrophilic superdelocalizability of atom 15, S_{2}^{E}(HOMO-1)* is the electrophilic superdelocalizability of the second highest molecular orbital localized on atom 2, Q_2 is the net charge of atom 2 and S_{7}^{N}(LUMO+2)* is the nucleophilic superdelocalizability of the third lowest empty MO localized on atom 7 (see Fig. 2).Tables 4 and 5 show the beta coefficients, the results of the t-test for significance of variable and the matrix of squared correlation coefficients for the variables of Eq. 2. There are no significant internal correlations between independent variables (Table 5). Figure 4 displays the plot of observed *vs.* calculated $\log(K_i)$.

Table 4: Beta coefficients and t-test for significance of coefficients in Eq. 2

	Beta	t(18)	p-level
S_{15}^{E}	0.94	11.27	0.000000
S_{2}^{E}(HOMO-1)*	0.46	5.32	0.00005
Q_2	0.26	3.29	0.004
S_{7}^{N}(LUMO+2)*	0.25	3.07	0.007

Table 5: Matrix of squared correlation coefficients for the variables in Eq. 2

	S_{15}^{E}	S_{2}^{E}(HOMO-1)*	Q_2	S_{7}^{N}(LUMO+2)*
S_{15}^{E}	1.00			
S_{2}^{E}(HOMO-1)*	0.11	1.00		
Q_2	0.00	0.00	1.00	
S_{7}^{N}(LUMO+2)*	0.00	0.08	0.00	1.00

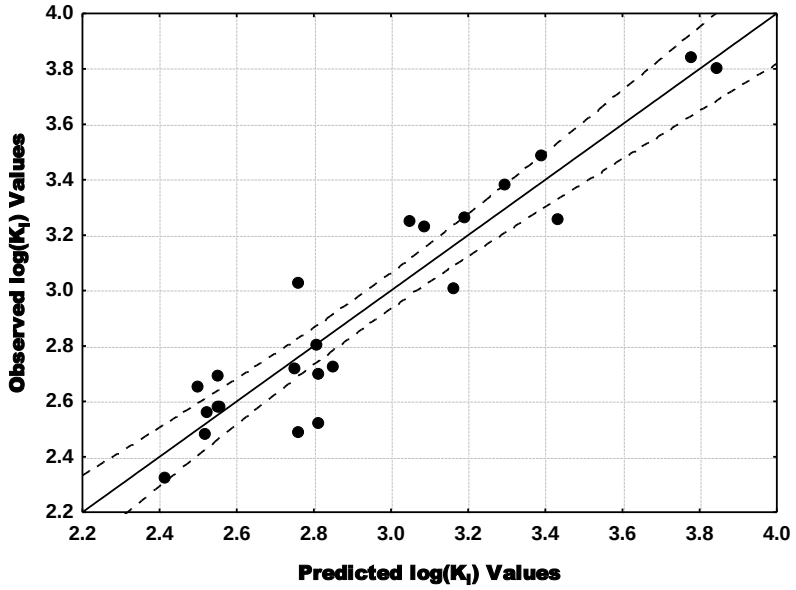

Figure 4: Plot of predicted vs. observed log(K_i). values (Eq. 2). Dashed lines denote the 95% confidence interval

The associated statistical parameters of Eq. 2 indicate that this equation is statistically significant and that the variation of the numerical values of a group of four local atomic reactivity indices of atoms of the common skeleton

explains about 87% of the variation of $\log(K_i)$. Figure 4, spanning about 1.4 orders of magnitude, shows that there is a relatively good correlation of observed *versus* calculated values.

Results for A_3AR receptors.

The best statistically significant equation obtained is the following:

$$\log(K_i)=-53.54+87.10Q_5-2.44\mu_{17}+0.26S_4^E(\text{HOMO-2})^*+2.87Q_{15}-12.96Q_9 \quad (3)$$

with n=23, R=0.97, R^2=0.94, adj-R^2=0.92, F(5,17)=49.26 ($p<0.000001$) and a standard error of the estimate of 0.17. No outliers were detected and no residuals fall outside the $\pm 2\sigma$ limits. Here, Q_5 is the net charge of atom 5, μ_{17} is the local atomic electronic chemical potential of atom 17, S_4^E(HOMO-2)* is the electrophilic superdelocalizability of the third highest molecular orbital localized on atom 2, Q_{15} is the net charge of atom 15 and Q_9 is the net charge of atom 9 (see Fig. 2).Tables 6 and 7 show the beta coefficients, the results of the t-test for significance of variable and the matrix of squared correlation coefficients for the variables of Eq. 3. There are no significant internal correlations between independent variables (Table 7). Figure 5 displays the plot of observed *vs.* calculated $\log(K_i)$.

Table 6: Beta coefficients and t-test for significance of coefficients in Eq. 3

	Beta	t(17)	p-level
Q_5	0.56	8.10	0.000000
μ_{17}	-0.33	-4.93	0.0001
S_4^E(HOMO-2)*	0.41	5.68	0.00003
Q_{15}	0.28	4.06	0.0008
Q_9	-0.18	-2.63	0.02

Table 7: Matrix of squared correlation coefficients for the variables in Eq. 3

	Q_5	**μ_{17}**	**S_4^E(HOMO-2)***	**Q_{15}**	**Q_9**
Q_5	1.00				
μ_{17}	0.00	1.00			
S_4^E(HOMO-2)*	0.12	0.00	1.00		
Q_{15}	0.01	0.16	0.00	1.00	
Q_9	0.03	0.00	0.08	0.01	1.00

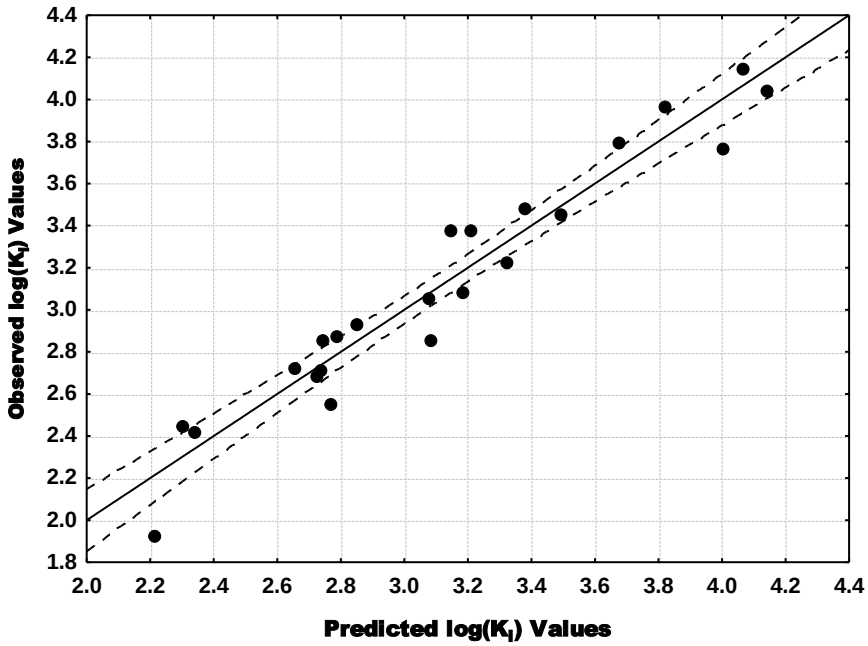

Figure 5: Plot of predicted vs. observed log(K_i) values (Eq. 3). Dashed lines denote the 95% confidence interval

The associated statistical parameters of Eq. 3 indicate that this equation is statistically significant and that the variation of the numerical values of a group of five local atomic reactivity indices of atoms of the common skeleton explains about 92% of the variation of $\log(K_i)$. Figure 5, spanning about 2 orders of magnitude, shows that there is a relatively good correlation of observed *versus* calculated values.

Local molecular orbitals

A very important point to stress is the following. When a local atomic reactivity index of an inner local occupied MO (i.e., (HOMO-1)* and/or (HOMO-2)*) or of a higher vacant MO ((LUMO+1)* and/or (LUMO+2)*) appears in any equation, this means that the remaining of the upper occupied MOs (for example, if (HOMO-2)* appears, upper means (HOMO-1)* and HOMO*) or the remaining of the empty MOs (for example, if (LUMO+1)* appears, lower means the LUMO*) contribute to the interaction. Their absence in the equation only means that the variation of their numerical values does not account for the variation of the numerical value of the biological property. Tables 8-10 show the local molecular orbitals of atoms 2, 4, 5, 6, 7, 9, 14, 15 and 17.Nomenclature for Tables: Molecule (HOMO) / (HOMO-2)* (HOMO-1)* (HOMO)* - (LUMO)* (LUMO+1)* (LUMO+2)*.

Table 8: Local molecular orbitals of atoms 2, 4 and 5

Mol.	2 (N)	4 (N)	5 (C)
1 (59)	57π58σ59π-62π63π66σ	57π58σ 59π-60π62π63π	57π58σ59π-62π63π64π
2 (63)	61π62σ63π-64π66π67π	61π62σ63π-64π66π67π	61π62σ63π-64π66π68π
3 (67)	65π66σ67π-70π71π72π	65π66σ67π-68π70π71π	65π66σ67π-70π71π72π
4 (74)	72σ73π74π-77π78π87π	72σ73π74π-75π77π78π	72σ73π74π-77π78π79π
5 (78)	76σ77π78π-81π82π83π	76σ77π78π-79π81π82π	76σ77π78π-81π82π83π
6 (82)	80σ81π82π-85π86π87π	80σ81π82π-83π85π86π	80σ81π82π-85π86π87π
7 (78)	76σ77π78π-81π82π92π	76σ77π78π-79π81π82π	76σ77π78π-81π82π83π
8 (82)	80π81π82π-85π86π87π	80π81π82π-83π85π86π	80π81π82π-85π86π87π
9 (86)	84π85π86π-89π90π91π	84π85π86π-87π89π90π	84π85π86π-89π90π91π
10 (78)	76π77π78π-81π82π92π	76π77π78π-79π81π82π	76π77π78π-81π82π83π
11 (82)	80σ81π82π-85π86π87π	80σ81π82π-83π85π86π	80σ81π82π-85π86π87π
12 (86)	84σ85π86π-89π90π91π	84σ85π86π-87π89π90π	83σ85π86π-89π90π91π
13 (82)	80σ81π82π-85π86π97π	80σ81π82π-83π85π86π	80σ81π82π-85π86π87π
14 (86)	84σ85π86π-89π90π91π	84σ85π86π-87π89π90π	84σ85π86π-89π90π91π
15 (90)	88π89π90π-93π94π95π	88π89π90π-91π93π94π	88π89π90π-93π94π95π
16 (78)	76π77σ78π-81π82π91π	76π77σ78π-79π81π82π	76π77π78π-79π81π82π
17 (82)	80σ81π82π-85π86π87π	80σ81π82π-83π85π86π	80σ81π82π-85π86π87π
18 (82)	80σ81π82π-85π86π100σ	80σ81π82π-83π85π86π	80σ81π82π-85π86π87π
19 (82)	80σ81π82π-85π86π100σ	80σ81π82π-83π85π86π	80σ81π82π-85π86π87π
20 (86)	84π85σ86π-89π90π92π	84π85σ86π-87π89π90π	84π85σ86π-89π90π91π
22 (86)	84σ85π86π-89π90π92π	84σ85π86π-87π89π90π	84σ85π86π-87π89π90π
23 (82)	80σ81π82π-85π86π96π	80σ81π82π-83π85π86π	80σ81π82π-85π86π87π
24 (86)	84σ85π86π-89π90π103σ	84σ85π86π-87π89π90π	84σ85π86π-89π90π91π
25 (82)	80σ81π82π-85π86π97π	80σ81π82π-83π85π86π	80σ81π82π-85π86π87π
26 (89)	87σ88π89π-92π93π105π	87σ88π89π-90π92π93π	87σ88π89π-90π92π93π

Table 9: Local molecular orbitals of atoms 6, 7 and 9

Mol.	6 (C)	7 (N)	9 (N)
1 (59)	57π58σ59π-62π63π64π	57σ58σ 59π-60π63π64π	57π58σ59π-60π63π64π
2 (63)	61π62σ63π-66π67π68π	61σ62σ63π-64π67π68π	61π62σ63π-64π67π68π
3 (67)	65π66σ67π-70π71π72π	65σ66σ67π-68π71π72π	65π66σ67π-68π71π72π
4 (74)	72σ73π74π-77π78π79π	72σ73π74π-75π78π79π	72σ73π74π-75π78π79π
5 (78)	76σ77π78π-81π82π83π	76σ77σ78π-79π82π83π	76σ77π78π-79π82π83π
6 (82)	80σ81π82π-85π86π87π	80σ81σ82π-83π86π87π	80σ81π82π-83π86π87π
7 (78)	76σ77π78π-81π82π83π	76σ77π78π-79π82π83π	76σ77π78π-79π81π82π
8 (82)	80π81π82π-85π86π87π	80π81π82π-83π86π87π	80π81π82π-83π86π87π
9 (86)	84σ85π86π-89π90π91π	84σ85σ86π-87π90π91π	84π85π86π-87π90π91π
10 (78)	76σ77π78π-81π82π83π	75σ77π78π-79π82π83π	76π77π78π-79π81π82π

11 (82)	80σ81π82π-85π86π87π	80σ81π82π-83π86π87π	80π81π82π-83π85π86π
12 (86)	83σ85π86π-89π90π91π	84σ85π86π-87π90π91π	83σ85π86π-87π89π90π
13 (82)	80σ81π82π-85π86π87π	80σ81π82π-83π86π87π	80σ81π82π-83π85π86π
14 (86)	84σ85π86π-89π90π91π	84σ85σ86π-87π90π91π	84π85π86π-87π89π90π
15 (90)	88σ89π90π-93π94π95π	88σ89σ90π-91π94π95π	88π89π90π-91π93π94π
16 (78)	76π77π78π-81π82π83π	76π77σ78π-79π80π82π	76π77π78π-79π82π83π
17 (82)	80σ81π82π-85π86π87π	80σ81σ82π-83π86π87π	80π81π82π-83π86π87π
18 (82)	80σ81π82π-85π86π87π	80σ81σ82π-83π86π87π	80σ81π82π-83π86π87π
19 (82)	80σ81π82π-85π86π87π	80σ81π82π-83π86π87π	80σ81π82π-83π85π86π
20 (86)	84π85σ86π-89π90π92π	84π85σ86π-87π89π90π	84π85σ86π-87π89π90π
22 (86)	84σ85π86π-89π90π92π	84σ85π86π-87π90π92π	84σ85π86π-87π90π92π
23 (82)	80σ81π82π-85π86π87π	80σ81π82π-83π86π87π	80σ81π82π-83π85π86π
24 (86)	83π84σ86π-89π90π91π	83π84σ86π-87π90π91π	83π84σ85π-87π89π90π
25 (82)	79π80σ82π-85π86π88π	79π80σ82π-83π86π87π	79π80σ81π-83π85π86π
26 (89)	87σ88π89π-92π93π94π	87σ88π89π-90π92π93π	87π88π89π-90π92π93π

Table 10: Local molecular orbitals of atoms 14, 15 and 17

Mol.	**14 (C)**	**15 (C)**	**17 (H)**
1 (59)	55π56π57π-60π61π62π	56π57π59π-60π61π62π	44σ46σ58σ-65σ66σ68σ
2 (63)	59π60π61π-64π65π66π	60π61π63π-64π65π66π	45σ46σ62σ-69σ70σ73σ
3 (67)	63π64π65π-68π69π70π	64π65π67π-68π69π70π	47σ49σ66σ-74σ75σ78σ
4 (74)	70π71π73π-75π76π77π	72σ73π74π-75π76π77π	57σ67σ72σ-81σ82σ83σ
5 (78)	74π75π77π-79π80π81π	76π77π78π-79π80π81π	59π71σ76σ-85σ86σ87σ
6 (82)	78π79π81π-83π84π85π	80π81π82π-83π84π85π	62σ75σ80σ-89σ90σ91σ
7 (78)	74π75π77π-79π80π81π	76π77π78π-79π80π81π	68σ71σ76σ-84σ85σ86σ
8 (82)	78π79π81π-83π84π85π	80π81π82π-83π84π85π	72σ75σ80σ-88σ89σ90σ
9 (86)	82π83π85π-87π88π89π	84π85π86π-87π88π89π	76σ79σ84σ-93σ94σ95σ
10 (78)	73π74π77π-79π80π81π	75π77π78π-79π80π81π	60σ70σ75σ-84σ85σ86σ
11 (82)	77π78π81π-83π84π85π	79π81π82π-83π84π85π	63σ74σ79σ-89σ90σ94σ
12 (86)	81π82π85π-87π88π89π	83π85π86π-87π88π89π	64σ78σ83σ-93σ94σ95σ
13 (82)	78π79π81π-83π84π85π	80π81π82π-83π84π85π	65σ75σ80σ-88σ89σ90σ
14 (86)	82π83π85π-87π88π89π	84π85π86π-87π88π89π	68σ79σ84σ-92σ93σ94σ
15 (90)	86π87π89π-91π92π93π	88π89π90π-91π92π93π	71σ83σ88σ-96σ97σ98σ
16 (78)	73σ75σ76π-79π80π81π	76π77π78π-79π80π81π	67σ70σ77σ-84σ85σ86σ
17 (82)	77π78π79π-83π84π85π	80π81π82π-83π84π85π	72σ75σ80σ-88σ90σ91σ
18 (82)	78π79π81π-83π84π85π	80π81π82π-83π84π85π	72σ75σ80σ-88σ89σ90σ
19 (82)	78π79π81π-83π84π85π	79π81π82π-83π84π85π	72σ75σ80σ-88σ89σ90σ
20 (86)	81π82π83π-87π88π89π	83π84π86π-87π88π89π	75σ79σ85σ-93σ94σ95σ
22 (86)	81π82π85π-87π88π89π	83π85π86π-87π88π89π	75σ79σ84σ-93σ94σ95σ
23 (82)	78π79π81π-83π84π85π	79π81π82π-83π84π85π	72σ75σ80σ-88σ89σ90σ
24 (86)	82π85π86π-87π88π89π	83π85π86π-87π88π89π	75σ79σ84σ-92σ93σ94σ
25 (82)	79π81π82π-83π84π85π	79π81π82π-83π84π85π	72σ75σ80σ-89σ90σ91σ
26 (89)	85π86π88π-90π91π92π	87π88π89π-90π91π92π	77σ81σ87σ-95σ96σ97σ

Discussion.

Discussion of A_1AR receptor affinity [36]

Table 2 shows that the importance of variables in Eq. 1 isω_9> S_6^E(HOMO-1)*> φ_{R2}> S_{14}^E(HOMO-2)*. The analysis of Eq. 1 shows that a high affinity is associated with small (positive) values of ω_9, small (negative) values of S_6^E(HOMO-1)* and S_{14}^E(HOMO-2)* and with small values of φ_{R2}. Now we shall carry out the analysis by separate of each component of the QSAR equation.R_2 is the substituent attached to atom 9 (Fig. 2). Inspecting Table 1 allows us to suggest that a methyl group should be optimal for high affinity. Atom 9 is nitrogen in ring B (Fig. 2). Table 9

shows that $(HOMO)_9^*$ and $(LUMO)_9^*$ coincide with the molecule's frontier MOs in all cases. The local atomic electrophilicity of atom 9, ω_9, is defined as:

$$\omega_9 = \frac{\mu_9^2}{2\eta_9} \quad (4)$$

where μ_9 is the local atomic electronic chemical potential of atom 9 and η_9 is the local atomic hardness of the same atom. As we said before a high affinity is associated with small values for ω_9. To obtain these values for ω_9 we may diminish the local atomic chemical potential or augment the local atomic hardness. Both procedures cannot be employed simultaneously. From a mathematical point of view, diminishing the local atomic chemical potential is more effective. If we move up the $LUMO_9^*$ energy the value of η_9 will increase and the value of μ_9 will move towards the zero of energy. This action will produce a bad electron acceptor atom but will allow atom 9 to employ its frontier π electrons to interact with an electron-deficient center. Atom 6 is a carbon in rings A-B (Fig. 2). Table 6 shows that $(HOMO-1)_6^*$ has a π or σ character following the molecule. Small (negative) values of $S_6^E(HOMO-1)^*$ are associated with high affinity. The best way to obtain these values is by making more negative the $(HOMO-1)_6^*$ energy. If we do the same for $(HOMO)_6^*$ this atom becomes a bad electron donor. Therefore we suggest that atom 6 is interacting with an electron-rich site. Atom 14 is a carbon in ring C (Fig. 2). Table 10 shows that $(HOMO-2)_{14}^*$ has a π character in all molecules but one. $(HOMO-1)_{14}^*$ is in the same situation. $(HOMO)_{14}^*$ has a π character in all molecules. In 23 of the 26 molecules $(HOMO)_{14}^*$ does not coincide with the molecular HOMO. The best way to obtain these values is by making more negative the $(HOMO-2)_{14}^*$ energy. If we do the same for $(HOMO-1)_{14}^*$ and $(HOMO)_{14}^*$ this atom becomes a bad electron donor. The whole interaction seems to be orbital-controlled Therefore we suggest that atom 14 is interacting with an electron-rich site. All the above suggestions are depicted in the partial 2D pharmacophore of Fig. 6.

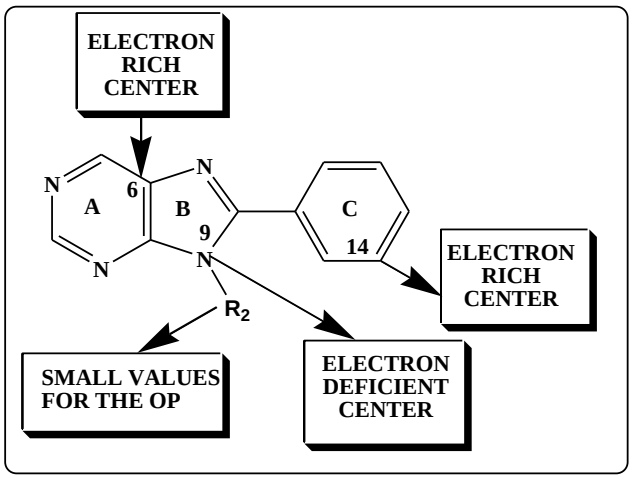

Figure 6: Partial 2D pharmacophore for A_1AR receptor affinity

Discussion of A_{2A}AR receptor affinity

Table 4 shows that the importance of variables in Eq. 2 is S_{15}^E>> $S_2^E(HOMO-1)^*$>> Q_2= $S_7^N(LUMO+2)^*$.The analysis of Eq. 2 shows that a high affinity is associated with high (negative) values for S_{15}^E and $S_2^E(HOMO-1)^*$, negative values for Q_2 and small positive values for $S_7^N(LUMO+2)^*$.Now we shall carry out the analysis by separate of each component of the QSAR equation. Atom 15 is a carbon in ring C (Fig. 2). Table 10 shows that all local frontier MOs (i.e., $HOMO_{15}^*$ and $LUMO_{15}^*$) coincide with the molecule's frontier orbitals and that all them have a π nature. A higher negative value for S_{15}^E is obtained by shifting upwards the occupied MO energies, especially from the three highest occupied local MOs because they are the dominant terms in the definition of the electrophilic superdelocalizability, local and total. Also this can be done by generating a degenerate $HOMO_{15}^*$ and/or a degenerate $(HOMO-1)_{15}$*. This problem can be solved only by quantum-chemical calculations of this molecule with

a large variety of substituents. We must note that we need to take care of the results because they can affect other variables appearing in Eq. 2. Then, we suggest that atom 15 is interacting with an electron-deficient center, probably of π nature. Atom 2 is nitrogen in ring A (Fig. 2). Table 8 shows that the local $HOMO_2$* coincides with the molecular HOMO and that the local $LUMO_2$* coincides with the molecular LUMO only in some molecules. Considering that high negative values for S_2^E(HOMO-1)* are associated with high affinity we may apply the same reasoning used for atom 15. We suggest that this atom is interacting with an electron-deficient center. This condition is consistent with the requirement of negative values for the net charge of this atom. Atom 7 is nitrogen in ring B (Fig. 2). Table 9 shows that all local frontier MOs have a π nature and that they coincide with the molecular frontier orbitals. Small positive values for S_7^N(LUMO+2)* are associated with a high affinity. These values are obtained by shifting upwards the MO energy, diminishing its electron-acceptance capacity. Therefore, we suggest that this atom also interacts with an electron-deficient center. The interaction seems to be charge- and orbital-controlled. All the above suggestions are depicted in the partial 2D pharmacophore of Fig. 7.

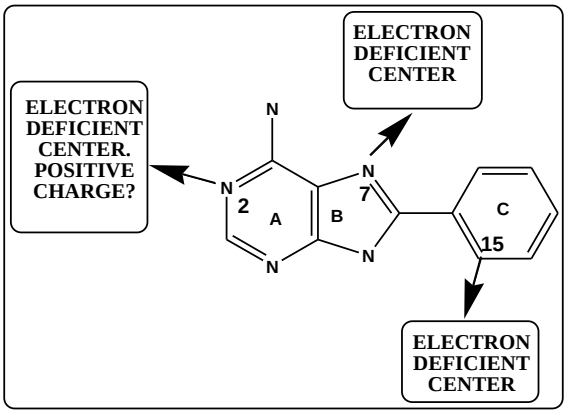

Figure 7: Partial 2D pharmacophore for A_{2A}AR receptor affinity

Discussion of A_3AR receptor affinity

Table 6 shows that the importance of variables in Eq. 3 is Q_5> S_4^E(HOMO-2)*> μ_{17}> Q_{15}> Q_9.The analysis of Eq. 3 shows that a high affinity is associated with a negative net charge on atom 5, a large (negative) value for μ_{17}, a high (negative) value for S_4^E(HOMO-2)*, a negative net charge on atom15 and a positive one on atom 9.Now we shall carry out the analysis by separate of each component of the QSAR equation. Atom 5 is a carbon belonging to rings A and B (Fig. 2). Table 8 shows that the local $HOMO_5^*$ coincides with the molecular HOMO in all cases. $LUMO_5^*$ coincides with the molecular LUMO in only four cases. All local MOs have a π nature. Given the situation of the frontier local MOs and the requirement of a negative net charge, we suggest that this atom is interacting with an electron deficient center that probably is positively charged. Note that Q_5 is the most significant variable in Eq. 3.Atom 4 is nitrogen in ring A (Fig. 2). Table 8 shows that all local frontier MOs, $HOMO_4$* and $LUMO_4$*, coincide with the molecular frontier MOs and that all them have a π nature. A large (negative) value for S_4^E(HOMO-2)* is associated with high affinity. Given that higher negative values are obtained by shifting upwards the MO energy (or by increasing the local MO population), the electron-donating capacity of this atom will be increased. Therefore, we suggest that atom 4 is interacting with an electron-deficient center. Atom 17 is the hydrogen bonded to N16 (Fig. 2). Table 10 shows that all MOs have σ nature. $HOMO_{17}$* is close to the molecular HOMO and $LUMO_{17}$*.A large (negative) value for μ_{17} is associated with high affinity. The local atomic electronic chemical potential is the midpoint of the $HOMO_{17}$* and $LUMO_{17}$* energies. The only way to get more negative values for this index is by suppressing the actual $HOMO_{17}$* in such a way that an inner occupied molecular MO becomes the new $HOMO_{17}$*. This will diminish the electron-donating capacity of atom 17. Now, the other way to help to obtain larger (negative) values for μ17 is by shifting downwards the local MO energy. This can be done by localizing the molecule's HOMO on atom 17. This, in turn, will increase the electron-acceptor capacity of this atom. This can be rationalized by

suggesting that atom 17 is participating in a hydrogen bond. Atom 15 is a carbon in ring C (Fig. 2). A negative net charge on this atom is associated with high affinity. This suggests an electrostatic interaction with a positively charged atom or group (ammonium for example).Atom 9 is nitrogen in ring B (Fig. 2). A positive net charge on this atom is associated with high affinity. This suggests an electrostatic interaction with a negatively charged atom or group (carboxylate for example).The interaction is also orbital- and charge-controlled. All the above suggestions are depicted in the partial 2D pharmacophore of Fig. 8.

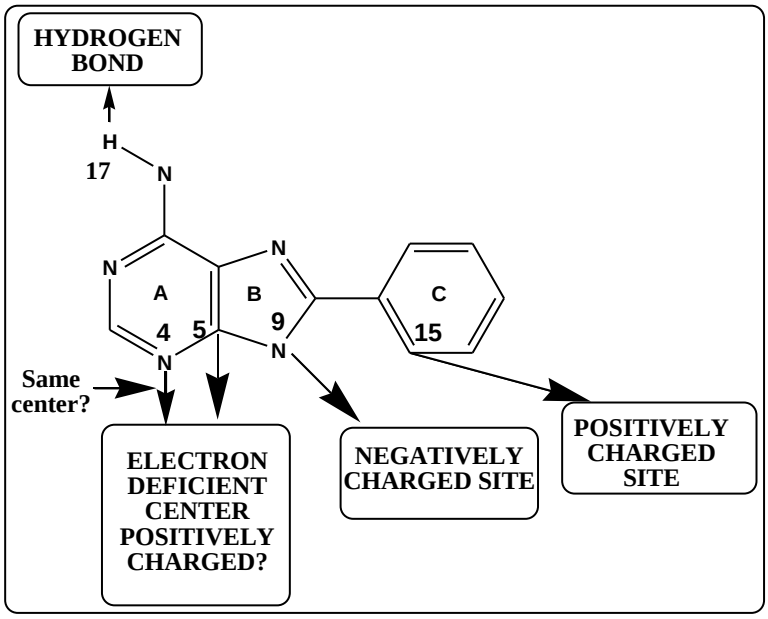

Figure 8: Partial 2D pharmacophore for A_3AR receptor affinity

In summary, we have obtained significant formal relationships between the electronic structure of a series of N^6-8,9-trisubstituted purine derivatives and their affinity for three adenosine receptors. The pharmacophores suggested here should be useful for quantum-chemical studies of new molecules with enhanced affinity. Also, it could serve as a guide for the synthesis of new molecules with enhanced or diminished receptor affinity.

References

[1]. Soliman, A. M.; Fathalla, A. M.; Moustafa, A. A. Adenosine role in brain functions: pathophysiological influence on Parkinson's disease and other brain disorders. *Pharmacological Reports* 2018.

[2]. Müller, C. E.; Baqi, Y.; Hinz, S.; Namasivayam, V. Medicinal Chemistry of A2B Adenosine Receptors. In *The Adenosine Receptors*, Borea, P. A.; Varani, K.; Gessi, S.; Merighi, S.; Vincenzi, F., Eds. Springer International Publishing: Cham, 2018; pp 137-168.

[3]. Jespers, W.; Schiedel, A. C.; Heitman, L. H.; Cooke, R. M.; Kleene, L.; van Westen, G. J. P.; Gloriam, D. E.; Müller, C. E.; Sotelo, E.; Gutiérrez-de-Terán, H. Structural Mapping of Adenosine Receptor Mutations: Ligand Binding and Signaling Mechanisms. *Trends in Pharmacological Sciences* 2018, 39, 75-89.

[4]. Jacobson, K. A.; Merighi, S.; Varani, K.; Borea, P. A.; Baraldi, S.; Aghazadeh Tabrizi, M.; Romagnoli, R.; Baraldi, P. G.; Ciancetta, A.; Tosh, D. K.; Gao, Z.-G.; Gessi, S. A3 Adenosine Receptors as Modulators of Inflammation: From Medicinal Chemistry to Therapy. *Medicinal Research Reviews* 2018, 38, 1031-1072.

[5]. Haskó, G.; Antonioli, L.; Cronstein, B. N. Adenosine metabolism, immunity and joint health. *Biochemical Pharmacology* 2018, 151, 307-313.

[6]. Borea, P. A.; Gessi, S.; Merighi, S.; Vincenzi, F.; Varani, K. Pharmacology of Adenosine Receptors: The State of the Art. *Physiological Reviews* 2018, 98, 1591-1625.

[7]. Antonioli, L.; Fornai, M.; Blandizzi, C.; Pacher, P.; Haskó, G. Adenosine signaling and the immune system: When a lot could be too much. *Immunology Letters* 2018.

[8]. Silva, L.; Subiabre, M.; Araos, J.; Sáez, T.; Salsoso, R.; Pardo, F.; Leiva, A.; San Martín, R.; Toledo, F.; Sobrevia, L. Insulin/adenosine axis linked signalling. *Molecular Aspects of Medicine* 2017, 55, 45-61.

[9]. Lambertucci, C.; Marucci, G.; Dal Ben, D.; Buccioni, M.; Spinaci, A.; Kachler, S.; Klotz, K.-N.; Volpini, R. New potent and selective A1 adenosine receptor antagonists as potential tools for the treatment of gastrointestinal diseases. *European Journal of Medicinal Chemistry* 2018, 151, 199-213.

[10]. Jacobson, K. A.; Tosh, D. K.; Gao, Z.-G.; Yu, J.; Suresh, R. R.; Rao, H.; Romagnoli, R.; Baraldi, P. G.; Aghazadeh Tabrizi, M. Medicinal Chemistry of the A3 Adenosine Receptor. In *The Adenosine Receptors*, Borea, P. A.; Varani, K.; Gessi, S.; Merighi, S.; Vincenzi, F., Eds. Springer International Publishing: Cham, 2018; pp 169-198.

[11]. Fonseca, A.; Matos, M. J.; Vilar, S.; Kachler, S.; Klotz, K.-N.; Uriarte, E.; Borges, F. Coumarins and adenosine receptors: New perceptions in structure–affinity relationships. *Chemical Biology & Drug Design* 2018, 91, 245-256.

[12]. Chandrasekaran, B.; Deb, P. K.; Kachler, S.; Akkinepalli, R. R.; Mailavaram, R.; Klotz, K.-N. Synthesis and adenosine receptors binding studies of new fluorinated analogues of pyrido[2,3-d]pyrimidines and quinazolines. *Medicinal Chemistry Research* 2018, 27, 756-767.

[13]. Catarzi, D.; Varano, F.; Falsini, M.; Varani, K.; Vincenzi, F.; Pasquini, S.; Dal Ben, D.; Colotta, V. Development of novel pyridazinone-based adenosine receptor ligands. *Bioorganic & Medicinal Chemistry Letters* 2018, 28, 1484-1489.

[14]. van der Walt, M. M.; Terre'Blanche, G. Selected C8 two-chain linkers enhance the adenosine A1/A2A receptor affinity and selectivity of caffeine. *European Journal of Medicinal Chemistry* 2017, 125, 652-656.

[15]. Peleli, M.; Fredholm, B. B.; Sobrevia, L.; Carlström, M. Pharmacological targeting of adenosine receptor signaling. *Molecular Aspects of Medicine* 2017, 55, 4-8.

[16]. Deb Pran, K.; Mailavaram, R.; Chandrasekaran, B.; Kaki Venkata, R.; Kaur, R.; Kachler, S.; Klotz, K. N.; Akkinepally Raghuram, R. Synthesis, adenosine receptor binding and molecular modelling studies of novel thieno[2,3-d]pyrimidine derivatives. *Chemical Biology & Drug Design* 2017, 91, 962-969.

[17]. Alachouzos, G.; Lenselink, E. B.; Mulder-Krieger, T.; de Vries, H.; Ijzerman, A. P.; Louvel, J. Synthesis and evaluation of N-substituted 2-amino-4,5-diarylpyrimidines as selective adenosine A1 receptor antagonists. *European Journal of Medicinal Chemistry* 2017, 125, 586-602.

[18]. Squarcialupi, L.; Falsini, M.; Catarzi, D.; Varano, F.; Betti, M.; Varani, K.; Vincenzi, F.; Dal Ben, D.; Lambertucci, C.; Volpini, R.; Colotta, V. Exploring the 2- and 5-positions of the pyrazolo[4,3-d]pyrimidin-7-amino scaffold to target human A1 and A2A adenosine receptors. *Bioorganic & Medicinal Chemistry* 2016, 24, 2794-2808.

[19]. Schenkel, L. B.; Olivieri, P. R.; Boezio, A. A.; Deak, H. L.; Emkey, R.; Graceffa, R. F.; Gunaydin, H.; Guzman-Perez, A.; Lee, J. H.; Teffera, Y.; Wang, W.; Youngblood, B. D.; Yu, V. L.; Zhang, M.; Gavva, N. R.; Lehto, S. G.; Geuns-Meyer, S. Optimization of a Novel Quinazolinone-Based Series of Transient Receptor Potential A1 (TRPA1) Antagonists Demonstrating Potent in Vivo Activity. *Journal of Medicinal Chemistry* 2016, 59, 2794-2809.

[20]. Van der Walt, M. M.; Terre'Blanche, G. 1,3,7-Triethyl-substituted xanthines—possess nanomolar affinity for the adenosine A1 receptor. *Bioorganic & Medicinal Chemistry* 2015, 23, 6641-6649.

[21]. Robinson, S. J.; Petzer, J. P.; Terre'Blanche, G.; Petzer, A.; van der Walt, M. M.; Bergh, J. J.; Lourens, A. C. U. 2-Aminopyrimidines as dual adenosine A1/A2A antagonists. *European Journal of Medicinal Chemistry* 2015, 104, 177-188.

[22]. Petrelli, R.; Torquati, I.; Kachler, S.; Luongo, L.; Maione, S.; Franchetti, P.; Grifantini, M.; Novellino, E.; Lavecchia, A.; Klotz, K.-N.; Cappellacci, L. 5′-C-Ethyl-tetrazolyl-N6-Substituted Adenosine and 2-Chloro-adenosine Derivatives as Highly Potent Dual Acting A1 Adenosine Receptor Agonists and A3 Adenosine Receptor Antagonists. *Journal of Medicinal Chemistry* 2015, 58, 2560-2566.

[23]. Giovannoni, M. P.; Ciciani, G.; Cilibrizzi, A.; Crocetti, L.; Daniele, S.; Di Cesare Mannelli, L.; Ghelardini, C.; Giacomelli, C.; Guerrini, G.; Martini, C.; Trincavelli, M. L.; Vergelli, C. Further studies on pyrazolo[1′,5′:1,6]pyrimido[4,5-d]pyridazin-4(3H)-ones as potent and selective human A1 adenosine receptor antagonists. *European Journal of Medicinal Chemistry* 2015, 89, 32-41.

[24]. Castelli, R.; Tognolini, M.; Vacondio, F.; Incerti, M.; Pala, D.; Callegari, D.; Bertoni, S.; Giorgio, C.; Hassan-Mohamed, I.; Zanotti, I.; Bugatti, A.; Rusnati, M.; Festuccia, C.; Rivara, S.; Barocelli, E.; Mor, M.; Lodola, A. Δ5-Cholenoyl-amino acids as selective and orally available antagonists of the Eph–ephrin system. *European Journal of Medicinal Chemistry* 2015, 103, 312-324.

[25]. Squarcialupi, L.; Colotta, V.; Catarzi, D.; Varano, F.; Betti, M.; Varani, K.; Vincenzi, F.; Borea, P. A.; Porta, N.; Ciancetta, A.; Moro, S. 7-Amino-2-phenylpyrazolo[4,3-d]pyrimidine derivatives: Structural investigations at the 5-position to target human A1 and A2A adenosine receptors. Molecular modeling and pharmacological studies. *European Journal of Medicinal Chemistry* 2014, 84, 614-627.

[26]. Li, A.-H.; Moro, S.; Forsyth, N.; Melman, N.; Ji, X.-d.; Jacobson, K. A. Synthesis, CoMFA Analysis, and Receptor Docking of 3,5-Diacyl-2,4-Dialkylpyridine Derivatives as Selective A3 Adenosine Receptor Antagonists. *Journal of Medicinal Chemistry* 1999, 42, 706-721.

[27]. Bondavalli, F.; Botta, M.; Bruno, O.; Ciacci, A.; Corelli, F.; Fossa, P.; Lucacchini, A.; Manetti, F.; Martini, C.; Menozzi, G.; Mosti, L.; Ranise, A.; Schenone, S.; Tafi, A.; Trincavelli, M. L. Synthesis, Molecular Modeling Studies, and Pharmacological Activity of Selective A1 Receptor Antagonists. *Journal of Medicinal Chemistry* 2002, 45, 4875-4887.

[28]. Note. The results presented here are obtained from what is now a routinary procedure. For this reason, we built a general model for the paper's structure. This model contains *standard* phrases for the presentation of the methods, calculations and results because they do not need to be rewritten repeatedly and the number of possible variations to use is finite. In 2017.

[29]. Gómez Jeria, J. S. La Pharmacologie Quantique. *Bollettino Chimico Farmaceutico* 1982, 121, 619-625.

[30]. Gómez-Jeria, J. S. On some problems in quantum pharmacology I. The partition functions. *International Journal of Quantum Chemistry* 1983, 23, 1969-1972.

[31]. Gómez-Jeria, J. S. Modeling the Drug-Receptor Interaction in Quantum Pharmacology. In *Molecules in Physics, Chemistry, and Biology*, Maruani, J., Ed. Springer Netherlands: 1989; Vol. 4, pp 215-231.

[32]. Gómez-Jeria, J. S.; Ojeda-Vergara, M. Parametrization of the orientational effects in the drug-receptor interaction. *Journal of the Chilean Chemical Society* 2003, 48, 119-124.

[33]. Gómez-Jeria, J. S. *Elements of Molecular Electronic Pharmacology (in Spanish)*. 1st ed.; Ediciones Sokar: Santiago de Chile, 2013; p 104.

[34]. Gómez-Jeria, J. S. A New Set of Local Reactivity Indices within the Hartree-Fock-Roothaan and Density Functional Theory Frameworks. *Canadian Chemical Transactions* 2013, 1, 25-55.

[35]. Gómez-Jeria, J. S. 45 Years of the KPG Method: A Tribute to Federico Peradejordi. *Journal of Computational Methods in Molecular Design* 2017, 7, 17-37.

[36]. Gómez-Jeria, J. S.; Kpotin, G. Some Remarks on The Interpretation of The Local Atomic Reactivity Indices Within the Klopman-Peradejordi-Gómez (KPG) Method. I. Theoretical Analysis. *Research Journal of Pharmaceutical, Biological and Chemical Sciences* 2018, 9, 550-561.

[37]. Kpotin, G.; Gómez-Jeria, J. S. Quantum-Chemical Study of the Relationships between Electronic Structure and Anti-Proliferative Activities of Quinoxaline Derivatives on the K562 and MCF-7 Cell Lines. *Chemistry Research Journal* 2018, 3, 20-33.

[38]. Gómez-Jeria, J. S.; Moreno-Rojas, C.; Castro-Latorre, P. A note on the binding of N-2-methoxybenzyl-phenethylamines (NBOMe drugs) to the 5-HT_{2C} receptors. *Chemistry Research Journal* 2018, 3, 169-175.

[39]. Gómez-Jeria, J. S.; Castro-Latorre, P.; Moreno-Rojas, C. Dissecting the drug-receptor interaction with the Klopman-Peradejordi-Gómez (KPG) method. II. The interaction of 2,5-dimethoxyphenethylamines and their N-2-methoxybenzyl-substituted analogs with 5-HT_{2A} serotonine receptors. *Chemistry Research Journal* 2018, 4, 45-62.

[40]. Kpotin, G.; Gómez-Jeria, J. S. A Quantum-chemical Study of the Relationships Between Electronic Structure and Anti-proliferative Activity of Quinoxaline Derivatives on the HeLa Cell Line. *International Journal of Computational and Theoretical Chemistry* 2017, 5, 59-68.

[41]. Gómez-Jeria, J. S.; Surco-Luque, J. C. A Quantum Chemical Analysis of the Relationships between Electronic Structure and the inhibition of Botulinum Neurotoxin serotype A by a series of Derivatives possessing an 8-hydroxyquinoline core. *Chemistry Research Journal* 2017, 2, 1-11.

[42]. Gómez-Jeria, J. S.; Moreno-Rojas, C. Dissecting the drug-receptor interaction with the Klopman-Peradejordi-Gómez (KPG) method. I. The interaction of 2,5-dimethoxyphenethylamines and their N-2-methoxybenzyl-substituted analogs with 5-HT1A serotonine receptors. *Chemistry Research Journal* 2017, 2, 27-41.

[43]. Gómez-Jeria, J. S.; Castro-Latorre, P.; Kpotin, G. Quantum Chemical Study of the Relationships between Electronic Structure and Antiviral Activities against Influenza A H1N1, Enterovirus 71 and Coxsackie B3 viruses of some Pyrazine-1,3-thiazine Hybrid Analogues. *International Journal of Research in Applied, Natural and Social Sciences* 2017, 5, 49-64.

[44]. Gómez-Jeria, J. S.; Castro-Latorre, P. A Density Functional Theory analysis of the relationships between the Badger index measuring carcinogenicity and the electronic structure of a series of substituted Benz[a]anthracene derivatives. *Chemistry Research Journal* 2017, 2, 112-126.

[45]. Gómez-Jeria, J. S.; Becerra-Ruiz, M. B. Electronic structure and rat fundus serotonin receptor binding affinity of phenetylamines and indolealkylamines. *International Journal of Advances in Pharmacy, Biology and Chemistry* 2017, 6, 72-86.

[46]. Gómez-Jeria, J. S.; Abuter-Márquez, J. A Theoretical Study of the Relationships between Electronic Structure and 5-HT_{1A} and 5- HT_{2A} Receptor Binding Affinity of a group of ligands containing an isonicotinic nucleus. *Chemistry Research Journal* 2017, 2, 198-213.

[47]. Anatovi, W.; Kpotin, G.; Kuevi, U. A.; Houngue-Kpota, A.; Atohoun, G. S.; Mensah, J.-B.; Gómez-Jeria, J. S. A DFT study or the relationship between the electronic structure and the antiplasmodial activity of a series of 4-anilino-2-trichloromethylquinazolines derivatives. *World Scientific News* 2017, 88, 138-151.

[48]. Robles-Navarro, A.; Gómez-Jeria, J. S. A Quantum-Chemical Analysis of the Relationships between Electronic Structure and Citotoxixity, GyrB inhibition, DNA Supercoiling inhibition and anti-tubercular activity of a series of quinoline–aminopiperidine hybrid analogues. *Der Pharma Chemica* 2016, 8, 417-440.

[49]. Kpotin, G. A.; Atohoun, G. S.; Kuevi, U. A.; Houngue-Kpota, A.; Mensah, J.-B.; Gómez-Jeria, J. S. A quantum-chemical study of the relationships between electronic structure and anti-HIV-1 activity of a series of HEPT derivatives. *Journal of Chemical and Pharmaceutical Research* 2016, 8, 1019-1026.

[50]. Kpotin, G.; Atohoun, S. Y. G.; Kuevi, U. A.; Kpota-Hounguè, A.; Mensah, J.-B.; Gómez-Jeria, J. S. A Quantum-Chemical study of the Relationships between Electronic Structure and Trypanocidal Activity against Trypanosoma Brucei Brucei of a series of Thiosemicarbazone derivatives. *Der Pharmacia Lettre* 2016, 8, 215-222.

[51]. Gómez-Jeria, J. S.; Salazar, R. A DFT study of the inhibition of FMS-like tyrosine kinase 3 and the antiproliferative activity against MV4-11 cells by N-(5-(tert-butyl)isoxazol-3-yl)-N'-phenylurea analogs. *Der Pharma Chemica* 2016, 8, 1-9.

[52]. Gómez-Jeria, J. S.; Orellana, Í. A theoretical analysis of the inhibition of the VEGFR-2 vascular endothelial growth factor and the anti-proliferative activity against the HepG2 hepatocellular carcinoma cell line by a series of 1-(4-((2-oxoindolin-3-ylidene)amino)phenyl)-3-arylureas. *Der Pharma Chemica* 2016, 8, 476-487.

[53]. Gómez-Jeria, J. S.; Moreno-Rojas, C. A theoretical study of the inhibition of human 4-hydroxyphenylpyruvate dioxygenase by a series of pyrazalone-quinazolone hybrids. *Der Pharma Chemica* 2016, 8, 475-482.

[54]. Gatica-Díaz, F.; Gómez-Jeria, J. S. A Theoretical Study of the Relationships between Electronic Structure and Cytotoxicity of a group of N^2-alkylated Quaternary β-Carbolines against nine Tumoral Cell Lines. *Journal of Computational Methods in Molecular Design* 2014, 4, 79-120.

[55]. Reyes-Díaz, I.; Gómez-Jeria, J. S. Quantum-chemical modeling of the hepatitis C virus replicon inhibitory potency and cytotoxicity of some pyrido[2,3-d]pyrimidine analogues. *Journal of Computational Methods in Molecular Design* 2013, 3, 11-21.

[56]. Gómez-Jeria, J. S.; Sotomayor, P. Quantum chemical study of electronic structure and receptor binding in opiates. *Journal of Molecular Structure: THEOCHEM* 1988, 166, 493-498.

[57]. Gómez-Jeria, J. S.; Morales-Lagos, D. R. Quantum chemical approach to the relationship between molecular structure and serotonin receptor binding affinity. *Journal of Pharmaceutical Sciences* 1984, 73, 1725-1728.

[58]. Gómez-Jeria, J. S.; Morales-Lagos, D. The mode of binding of phenylalkylamines to the Serotonergic Receptor. In *QSAR in design of Bioactive Drugs*, Kuchar, M., Ed. Prous, J.R.: Barcelona, Spain, 1984; pp 145-173.

[59]. Frisch, M. J.; Trucks, G. W.; Schlegel, H. B.; Scuseria, G. E.; Robb, M. A.; Cheeseman, J. R.; Montgomery, J., J.A.; Vreven, T.; Kudin, K. N.; Burant, J. C.; Millam, J. M.; Iyengar, S. S.; Tomasi, J.; Barone, V.; Mennucci, B.; Cossi, M.; Scalmani, G.; Rega, N. *G03 Rev. E.01*, Gaussian: Pittsburgh, PA, USA, 2007.

[60]. Gómez-Jeria, J. S. *D-Cent-QSAR: A program to generate Local Atomic Reactivity Indices from Gaussian 03 log files. v. 1.0*, v. 1.0; Santiago, Chile, 2014.

[61]. Gómez-Jeria, J. S. An empirical way to correct some drawbacks of Mulliken Population Analysis (Erratum in: J. Chil. Chem. Soc., 55, 4, IX, 2010). *Journal of the Chilean Chemical Society* 2009, 54, 482-485.

[62]. Gómez-Jeria, J. S. *STERIC: A program for calculating the Orientational Parameters of the substituents* 2.0; Santiago, Chile, 2015.

[63]. Statsoft. *Statistica v. 8.0*, 2300 East 14 th St. Tulsa, OK 74104, USA, 1984-2007.